Optimization of Vortex Generator Placement for Enhanced NACA 2412 Airfoil Performance – A Numerical Study

YAGYA DUTTA DWIVEDI, ANWAR BAIG
Department of Aeronautical Engineering,
Institute of Aeronautical Engineering,
Dundigal, Hyderabad, 500043, Telangana,
INDIA

Abstract: - There are four fundamental forces on aircraft when it flies: lift, drag, thrust, and weight. For an Aircraft to fly, its wings generate sufficient lift to overcome the weight of the aircraft. The wings are the main components that generate enough lift by their shape called an airfoil. A common technique to boost lift is introducing turbulence, having more kinetic energy, keeping the airflow attached to the wing longer near the trailing edge of the wing. Thus, this delays the separation over the wing. The increased momentum in the boundary layer allows it to handle adverse pressure gradients, and adding a turbulence generator on its uppermost layer increases the lift significantly. A vortex generator is a particular tool that helps in accelerating the change from a smooth to a turbulent boundary layer. Applying Computational Fluid Dynamics (CFD) analysis, this study analyses the effects of vortex generators on the NACA-2412 airfoil's aerodynamic performance. The main objective is to study the impact of applying straight-type vortex generators on the lift coefficient. This can be achieved by comparing an airfoil with vortex generators at different angles of attack. The vortex generators are located between 15 and 30% of the chord length toward the leading edge, and the angles of attack used are -5, -10, 0º, 5º, and 10º. The data indicate that the lift coefficient is greater with the vortex generator than with a normal airfoil and increases with angle of attack. The greatest improvement was observed at 5º, where the lift increased by 8–13%. By decreasing drag, the amount of thrust reduces fuel consumption, and emission is reduced, this improvement could improve sustainability and efficiency of the system.

Key-Words: - Computational fluid dynamics, Vortex generator, NACA, Angle of attack, airfoil, lift, drag.

Received: February 17, 2026. Revised: April 19, 2026. Accepted: June 29, 2026. Published: November 6, 2026.

1 Introduction

The rapidly developing wind energy sector is focused on creating larger and more powerful wind turbines that can supply the world's growing demand for clean energy while reducing environmental damage. Modern turbine blades are becoming longer, lighter, and slenderer in order to collect more wind and generate more power [1]. These designs, however, present major aerodynamic issues due to their higher adaptability and susceptibility to unpredictable wind conditions, including gusts, wind shear, yaw angles, and quick pitch changes. One key challenge is dynamic stall, which occurs when the wind angle changes quickly, leading airflow to separate from the blade at higher angles than in steady winds and attach more slowly [2]. This generates sudden lift increases that are followed by sharp drops, resulting in vibrations, greater drag, and fatigue loading, which may reduce the structural life of the blades [3]. As blades grow longer and more flexible, they become more susceptible to dynamic stall, which is an essential factor in current blade design. To address this, researchers suggested the use of vortex generators (VGs) and Gurney flaps (GFs) as passive flow control devices. VGs are small fins affixed to the blade surface that form swirling air patterns (vortices), which improve the boundary layer and allow the airflow to remain connected for a longer period of time. This decreases stall, increases lift, and improves aerodynamic stability, especially in dynamic conditions [4]. However, design factors like shape, height, angle, spacing, and chord wise location have an important effect on VG performance. VGs can potentially result in unstable loads or greater drag if they are not optimized [5]. The implementation of VGs with flat back airfoils—which have thick trailing edges for structural advantages and higher lift but additionally suffer from increased drag and noise has become the subject of much research. Performance can be improved by positioning VGs close to the leading

edge and utilizing gothic or triangular shapes, based on experimental tests performed using particle image velocimetry (PIV), oil flow visualization, and wind tunnel data [6]. However, spacing needs to be optimized; VGs placed too close together interact with one another, while those placed too far apart lose effectiveness. Some studies have also shown that VG mounting strips may lead to early turbulence, increasing drag [7]. In addition to VGs, Gurney flaps, which are small tabs attached to the trailing edge, are used to increase the airfoil's effective camber and lift. GFs are especially effective on heavily cambered airfoils with moderate speeds or high angles of attack. According to research, small GFs can increase lift as well as reduce drag, whereas larger ones commonly result in excessive drag [8]. When GFs combine with VGs, the results are mixed. Because VGs increase stall angle and GFs improve lift, their combined use could decrease overall performance if not correctly tuned [9].

Various studies focused on dynamic flow situations in which the angle of attack changes continuously, corresponding to real turbine operation. These studies indicated that VGs not only improve lift and delay stall but also adjust the aerodynamic response loops, leading to more predicted blade forces. However, in other situations, VGs resulted in major lift overshoots, which can increase stress to the structure [10]. The effect of lowered frequency, which impacts how quickly the blade angle modifications occur, was also analysed. At higher reduction frequencies, unstable flow effects become stronger, and VGs play a larger role in maintaining airflow continuity and reducing the chances of flow separation. [11]. A constant finding across all 15 research projects reveals that there is no uniform VG or GF design that is suitable for all blade sections and situations. Each section of the blade, whether it is near the root, middle, or tip, necessitates a customized solution based on blade shape and operating conditions [12]. Some studies also analysed the effect of VG geometry, concluding that gothic VGs improve lift more than standard designs. Additionally, the connection between VGs and the normal flow separation is greatly influenced by the flow's Reynolds number, turbulence, and vortex behavior, requiring careful evaluation and modelling [13], [14]. Overall, the study shows that well-designed and properly located VGs and GFs can significantly enhance airfoil performance by increasing lift, delaying stall, and stabilizing flow behavior in dynamic situations. These improvements help to reduce structural fatigue, increase turbine life, and improve overall efficiency [15], [16]. However, if poorly constructed, these devices could cause damage rather than good through increasing drag, producing vibrations, or causing uneven blade loading [17]. The simulations analyse flow patterns and drying efficiency to improve heat and mass transfer performance. Results demonstrate CFD's effectiveness in enhancing dryer design through parameter optimization [18], [19]. The present work is used to optimize the vortex generator location on the upper surface of the wing for improvement in the aerodynamic characteristics such as high lift coefficient (C_l), Drag coefficient (C_d), and aerodynamic efficiency $\frac{C_l}{C_d}$.

2 Methodology

An overview of the analytical and experimental methods used to evaluate aerodynamic characteristics of the wing and how the vortex generators (VGs) on NACA 2412 are affecting its performance is presented in this section. All the figures in this work are created by authors using modelling tools.

2.1 Geometry and Model Preparation

The baseline NACA-2412 airfoil geometry was created in SolidWorks with accurate chord wise dimensions. Four airfoil models were designed, each with vortex generators placed at chordwise locations of 15%, 20%, 25%, and 30% from the leading edge. The VGs were straight-type, with a constant 1-meter height, and uniform spacing was maintained along the span for each model. These configurations are illustrated in Figure 1, Figure 2, Figure 3, Figure 4 and Table 1 gives the details of the VG's placed on the wing design.

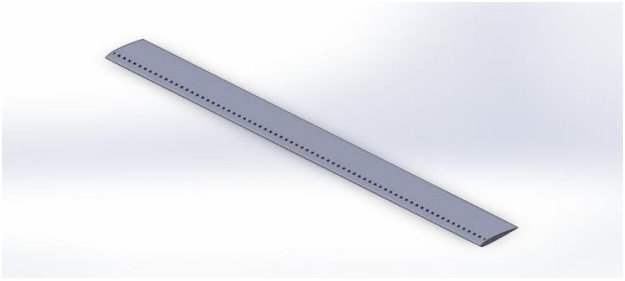


Fig. 1: VG positioned at 15% of the chord on a wing of 1 m span
Source: created by authors

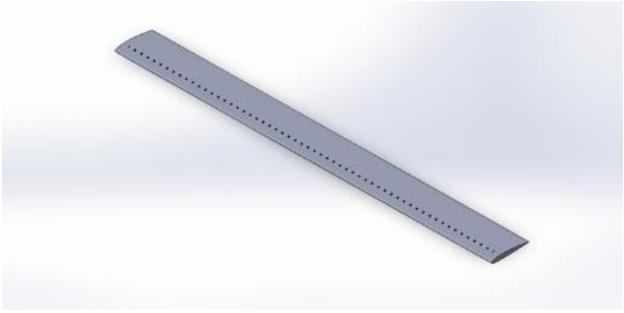


Fig. 2: VG positioned at 20% of the chord on a wing of 1 m span
Source: created by authors

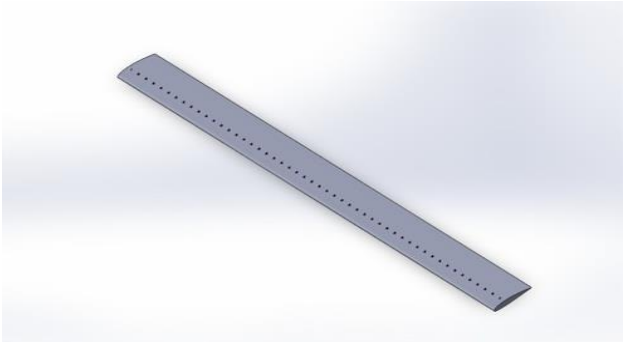


Fig. 3: VG positioned at 25% of the chord on a wing of 1 m span
Source: created by authors

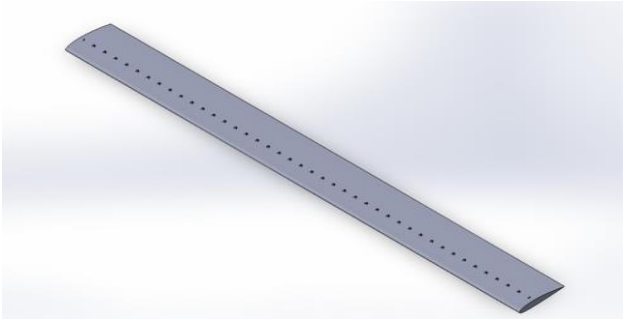


Fig. 4: VG positioned at 30% of the chord on a wing of 1 m span
Source: created by authors

Table 1. VG positioning and height configurations

VG Placement Along Chord (%)	VG Height (mm)	Description
15	2.32	VG at 15% chord
20	2.32	VG at 20% chord
25	2.32	VG at 25% chord
30	2.32	VG at 30% chord

Source: created by authors

2.2 Fabrication and Validation

Each model has been developed utilizing high-resolution 3D printing techniques to provide high dimensional accuracy and geometric fidelity, as specified in the CAD models (Figure 5 and Figure 6). Dimensional verification was performed after fabrication using calibrated instruments to ensure that the design criteria were matched. This process ensures the dependability of following aerodynamic testing. The details and positioning of the vortex generators on the wing of airfoil NACA-2412 with a rectangular cross-section are given in Table 2.

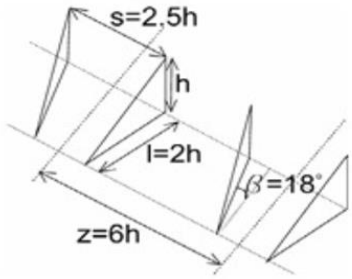


Fig. 5: Sketch of vortex generator geometry
Source: created by authors

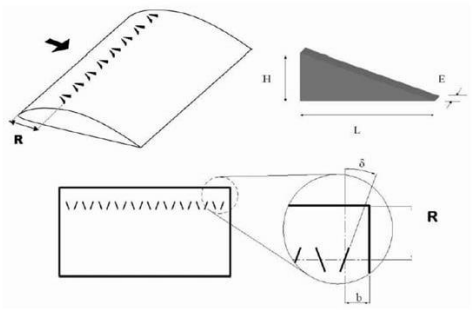


Fig. 6: Geometric parameters for the VG's
Source: created by authors

Table 2. Placements and VG

Parameter	Range	Units
l	4.64	mm
H	2.32	mm
E	0.464	mm
β	18	° (degree)
S	5.8	Mm
Z	13.92	Mm
X	15%C,20%C,25%C,30%C	Mm

Source: created by authors

2.3 Experimental Procedure

Experiments were conducted in a closed-circuit wind tunnel facility available at IARE Aerodynamics laboratory with a calibrated six-component force balance. Testing conditions included freestream velocities ranging from 10 to 30 m/s at a constant angle of attack of 5º. Each configuration was tested five times to ensure repeatability and reliability of the experimental results.

Test Parameters

The experimental conditions were accurately controlled for the wind tunnel tests. The primary AoA was maintained at a constant 5^0 . The investigation spanned a range of freestream velocities from 10 to 30 m/s. Under these conditions, the flow analysis operated at a characteristic Reynolds Number (Re) of approximately 1.5×10^5 . For aerodynamic coefficient calculations, the Air Density (ρ) was fixed at 1.225 kg/m^3 , utilizing a Reference Area (A) of 20 m^2. This consistent parameter set was crucial for ensuring the reliability of the comparative performance evaluation.

2.4 Mathematical Equations for Aerodynamic Analysis

Lift coefficient (C_L) and drag coefficient (C_D), were computed as given in Eq, (1) and (2) respectively:

$$C_L = \frac{2L}{\rho U^2 S} \tag{1}$$

$$C_D = \frac{2D}{\rho U^2 S} \tag{2}$$

where:
L = lift force in N
D = drag force in N
ρ = density of air in kg/m^3
U = free stream velocity in m/s
S = surface area viewed from top in m^2

The Reynold's number (Re) is calculated as given in Eq. (3), taking chord as the reference length

$$Re = \frac{\rho UL}{\mu} \tag{3}$$

where:
μ = viscosity in Pa-s
L = chord length in m

RANS equation 4, provides an excellent balance of accuracy and cost for most airfoil simulations. All terms related to RANS equations are given in Table 3. It's the workhorse of aerodynamic design, capable of predicting lift, drag, and flow patterns with sufficient accuracy for engineering purposes, while being fast enough for parametric studies and optimization.

$$\rho\left(\frac{\partial \overline{u_i}}{\partial t} + \overline{u_j}\frac{\partial \overline{u_i}}{\partial x_j}\right) = -\frac{\partial \bar{p}}{\partial x_i} + \frac{\partial}{\partial x_j}\left[\mu\left(\frac{\partial \overline{u_i}}{\partial x_j} + \frac{\partial \overline{u_j}}{\partial x_i}\right) \underbrace{-\rho\overline{u_i' u_j'}}_{\text{Reynolds Stress}}\right] \tag{4}$$

Table 3. Explanation of terms of RANS equation (4)

Term	Description
$\rho\overline{u_j}\frac{\partial \overline{u_i}}{\partial x_j}$	Convective acceleration of the mean flow.
$-\frac{\partial \bar{p}}{\partial x_i}$	Mean pressure gradient force.
$\mu\frac{\partial^2 \overline{u_i}}{\partial x_j \partial x_j}$	Viscous diffusion (molecular viscosity).
$-\rho\overline{u_i' u_j'}$	Reynolds Stress Tensor: This term represents the transport of momentum due to turbulent fluctuations.

Source: created by authors

The Standard k-ε model is used for this work. It has two-equation RANS closure that solves for turbulent kinetic energy (k) and its dissipation rate (ε). It calculates turbulent viscosity as $\nu t = C\mu k^2/\varepsilon$. The transport equations for k and ε model their production, destruction, and diffusion. This model is Simple, robust, and computationally cheap for flows with high Reynolds numbers and weak pressure gradients. Transport Equation for Kinetic Energy (k) given in equation 5.

$$\frac{\partial(\rho k)}{\partial t} + \frac{\partial(\rho k U_i)}{\partial x_i} = \frac{\partial}{\partial x_j}\left[\left(\mu + \frac{\mu_t}{\sigma_k}\right)\frac{\partial k}{\partial x_j}\right] + P_k - \rho\epsilon + S_k \tag{5}$$

2.5 Validation and Repeatability

The Computational Fluid Dynamics (CFD) model, with the optimal Vortex Generators (VGs), was supported by the two-step procedure to find the accuracy of the final conclusion. The first phase is to establish the numerical correctness. The aerodynamic coefficients from the simulations were

compared with the experimental data results that had observed in the literature, which is verifying an accuracy of 3% and validating the methodology. The second stage of this will be focusing on the physical effect of the vortex generators which is the innovative part of this study. Here the simulations that obtained from the pressure and velocity contours, identified in the mechanism in the previous studies. The vortex generators created high-energy vortices into the boundary layer, which helped the pressure recovery in the downstream area. The correct prediction of pressure distribution and flow behavior especially the flow separation delay and the increasement of the stall margin which gives strong confidence in the ability of the improvement performance improvements due to the new VG placement through the model

3 Results and Discussion

3.1 Discussion of Pressure Contours

The qualitative aerodynamic performance is initially validated by the pressure distribution on the NACA 2412 airfoil, as seen in Figure 7. Figure 7(a) is the baseline of an airfoil at a certain angle of attack (AoA). In Figure 7(b), the airfoil will be a pressure reversal at higher AoA, where the low-pressure area will be shifting to the lower surface of the airfoil, producing a downward force. In Figure 7(c), the vortex generators permit the stable pressure pattern even at higher AoA. The most important aspect is found in Figure 7(d), which represents the optimal AoA, where the low pressure zone is on the upper surface. This is a clear representation of the VGs which will reduces the adverse pressure gradient and also allow pressure recovery that leads tothe reason for the enhancement of lift that can be seen here.

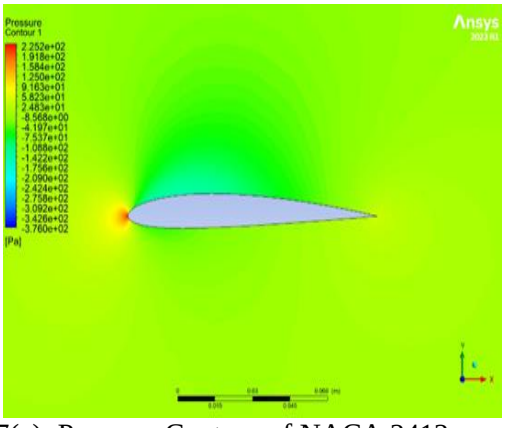


Fig. 7(a): Pressure Contour of NACA 2412
Source: created by authors

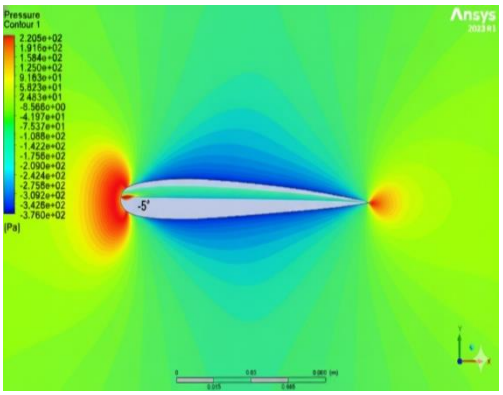


Fig. 7(b): Pressure Contour of NACA 2412 at -5^0 angle of attack
Source: created by authors

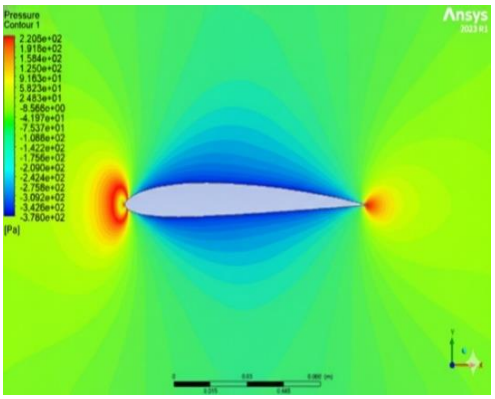


Fig. 7(c): Pressure Contour of NACA 2412 at 0^0 angle of attack
Source: created by authors

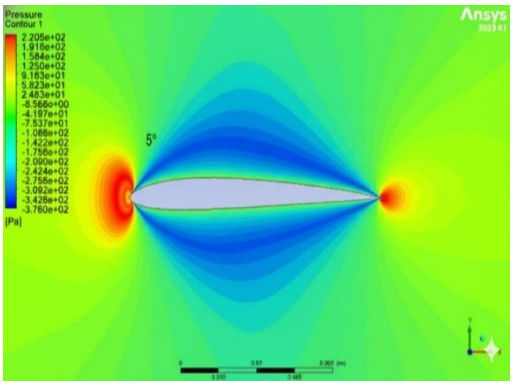


Fig. 7(d): Pressure Contour of NACA 2412 at 5^0 angle of attack
Source: created by authors

3.2 Aerodynamic Coefficient Analysis

The plots of coefficient of lift (C_l) and coefficient of drag (C_d) against angle of attack (AoA) allow us to evaluate the effect of vortex generators (VGs) on the overall aerodynamic performance of the airfoil.

In the lift curve of Figure 8a, all Vortex generators have a linear tendency of increasing values of the coefficient of lift with increasing angles of attack until the stall region. However, the

airfoil with vortex generators has a tendency to show coefficient of lift enhancement compared to the without vortex generators case, and this effect is more noticeable with increasing AoA.

Among the different vortex generator configurations analysed, the locations at 20% and 25% chord (0.2 and 0.25 c) placements show improvement of the coefficient of lift closer to the top region, which is attributed to the phenomenon of delayed separation.

The baseline airfoil begins to lose coefficient of lift earlier compared to the VG proposed cases, which are able to maintain lift for a greater range of AoA. This confirms the hypothesis that VGs do help to gain in kinetic energy on the boundary layer and allow the air to remain attached at greater angles of attack and up to more chord position.

With respect to the drag coefficient response (Figure 8b), the initial behavior of the drag coefficient with increased angles of attack is a decrease followed by a sharp increase at higher angles. At low angles, the baseline airfoil has the smallest drag values. This is expected as the vortex generator introduces enhanced surface disturbances. In contrast, at higher AoA, the VG cases have a more gradual increase in drag compared to the baseline case, which has a very steep increase. This indicates that VGs have a small negative effect on drag at lower angles, but help to control the increase of drag associated with flow separation at higher angles.

When comparing VG placements, the 15% chord position shows a relatively balanced performance with moderate lift improvement and relatively lower incremental drag. The 20% and 25% placements have better lift retention at high angles of attack (AoA), but with a small, incremental increase in drag.

The results demonstrate that vortex generators improve the aerodynamic performance of the airfoil, primarily in the high angles of attack region, by postponing the stall and controlling the flow. The placement of vortex generators is of utmost importance as it determines the lift enhancement and drag penalty balance.

The drag polar plot (C_l vs Cd) illustrates the aerodynamic efficiency of the airfoil with and without the vortex generators. This type of curve is quite helpful to understand how well the airfoil generates lift for a certain amount of drag (Figure 8c).

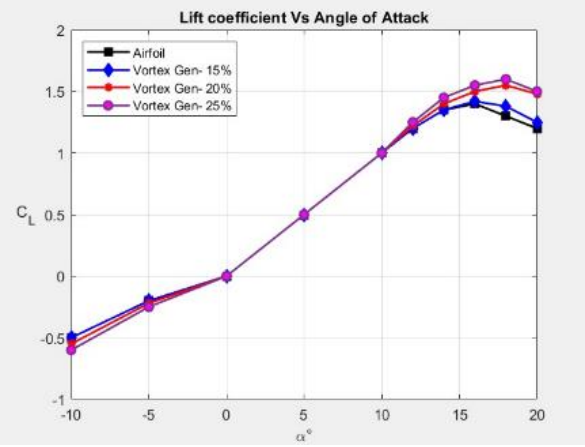
In the baseline case, the curve shows a normal trend with lift increasing along with drag. At low lift values, the airfoil is operating in a highly efficient region with low drag. However, at higher lift values, the drag increases substantially, indicating flow separation and higher aerodynamic losses. This limits efficiency, particularly in the high lift region.

With the drag coefficient, the lift-to-drag ratio (l/d) indicates a notable improvement. The VG airfoil planes achieve higher Cl for a small amount of added drag. While it may seem like a disadvantage, the primary point is that lift continues to increase without a sudden drop or deflection. This indicates delayed stall and flow attachment (8c).

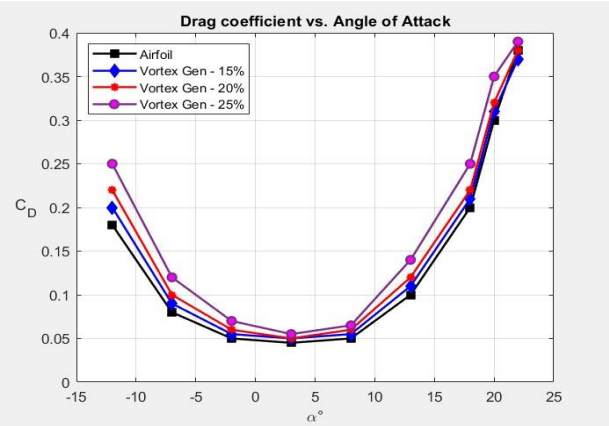
The 15% chord placement shows a very balanced shift in the curve with relatively low drag and positive lift. The 20% chord placement shows a more upward shift with an indication of more positive boundary layer control; however, some drag is noted with this positive shift. The 25% chord placement shows the highest potential positive shift, but at the cost of drag with delayed more violent vortex interaction.

Another observation is that the VG curves appear more smooth and much more extended than the baseline overall, implying more uniform and stable aerodynamic design with a steady extended operational range, in addition to the noted extended range and stability, the curve also appears to have a much gentler break, implying the stall becomes more of a gradual process and is much more favourable from an operational design purpose.

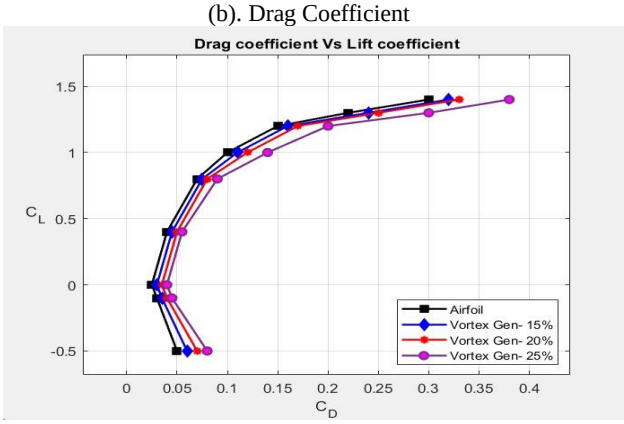
The drag polar confirms more lift, and the vortex generators improve the lift to drag ratio at higher levels of lift, and while the vortex generators design does incur a slight drag cost, in a design purpose from a lift standpoint of the plane, the vortex generators improve the design and overall performance at higher lift levels of the plane design in the aerodynamic design from a design plane design standpoint.



(a). Lift Coefficient vs AoA



(b). Drag Coefficient



(c). Lift to Drag Coefficient (Source: created by authors)

Fig. 8: Variation of aerodynamic characteristics CL, CD, Vs AoA (a, b) and CL vs CD plots (c)
Source: created by authors

3.3 Velocity Contour and Flow Field Analysis

The NACA 2412 airfoil CFD velocity contours portray the impact of vortex generators (VGs) on different chord-wise positions and angles of attack (AoA). In the baseline scenario (Figure 9a), the air velocity is high near the up-stream side and then becomes low toward the down-stream side. The low velocity is due to the formation of a thick boundary layer and the flow separation. A wider up-stream side recirculation zone, caused by a greater pressure drag, resulted in a decrease in the airfoil's aerodynamic efficiency.

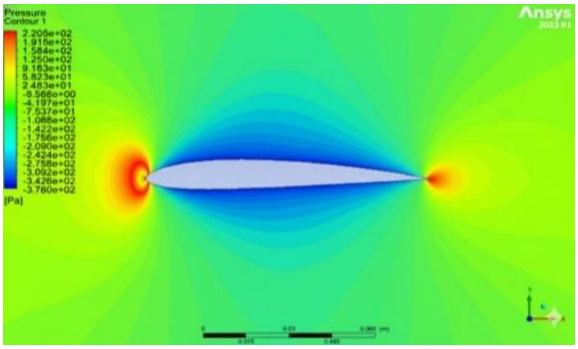
Introducing vortex generators at 15% of the chord and at AoA 5° (Figure 9b) improves the flow characteristics remarkably. The vortices produced contribute to the momentum exchange in the boundary layer, and separation is delayed.

This is visible through the reduction of the low-velocity zone over the upper surface and a more compact wake region. The sharper velocity gradient near the surface also suggests better momentum exchange and stronger flow attachment.

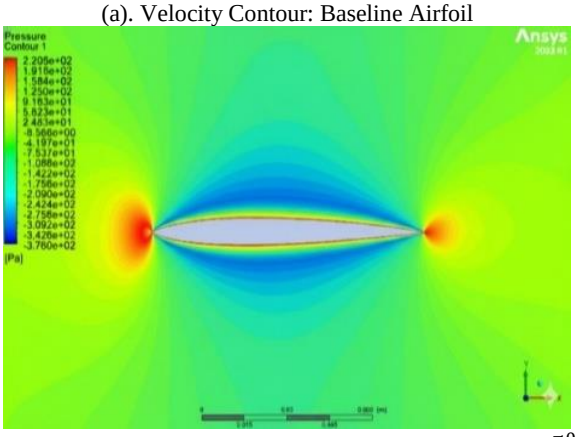
At 20% chord and a higher AoA of 20° (Figure 9c), the benefits of VGs become even more evident under stronger adverse pressure gradients. Although such high angles typically lead to early separation, the airflow remains attached over a larger portion of the airfoil. The wake remains relatively controlled, indicating that VGs are effective in maintaining lift by stabilizing the boundary layer even near stall conditions.

For the case with VGs placed at 25% chord and 25° AoA (Figure 9d), the improvement is still present but less effective compared to earlier placements. Since the VGs interact with the flow later, some separation occurs near the trailing edge, and the wake begins to widen again.

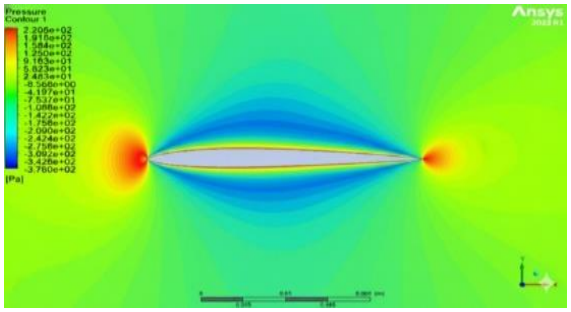
In summary, the analysis shows that vortex generators play a crucial role in improving flow attachment and reducing separation, with better performance achieved when they are positioned closer to the leading edge.



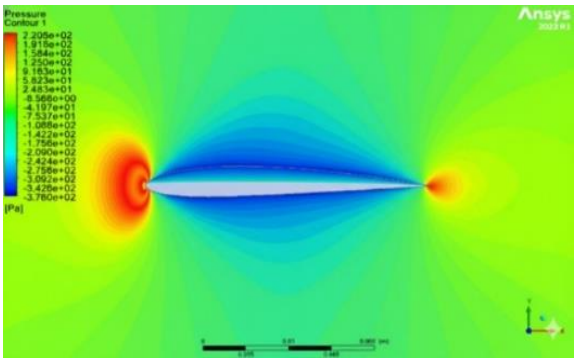
(a). Velocity Contour: Baseline Airfoil



(b). Velocity Contour: Airfoil with VGs at 15% Chord at 5^0 AoA



(c). Velocity Contour: Airfoil with VGs at 20 %Chord at 20^0AoA



(d). Velocity Contour: Airfoil with VGs at 25% Chord at 25^0 AoA

Fig. 9: Velocity Contour of NACA 2412
Source: created by authors

4 Conclusion

Numerical and experimental work was undertaken to find the effects of vortex generators on the NACA airfoil 2412 wing. The major findings show that the utilization of vortex generators significantly improves lift performance while causing a controlled increase in drag. Using VGs improves lift coefficient by 8-13% at a 5º angle of attack, with the ideal placement between 15% and 20% of chord length. The lift-to-drag ratio suggested greatest improvements at the 20% chord VG region, indicating improved aerodynamic performance. Vortex generators create strong vortex structures that energize the boundary layer and delay flow separation at angles of attack up to 25º, based on velocity contour

Pressure distribution graphs showed better pressure recovery downstream of the VGs, showing increased lift and stall margin extension. In qualitative terms, the analysis reveals that smart VG positioning and design effectively reduce adverse pressure gradients and flow separation, resulting in maintained interconnected flow and improved aerodynamic force stability. These enhancements help to improve aerodynamic dependability and the potential for fuel savings and decreases in emissions in aerospace and wind energy applications.

Overall, the continuous validation of CFD results with experimental measurements improves the modelling approach used. Future research may look into VG geometry optimization and unsteady flow effects to improve aerodynamic control and energy economy.

Declaration of Generative AI and AI-assisted Technologies in the Writing Process

During the preparation of this work, the author(s) utilized artificial intelligence (AI) technologies solely for the purpose of linguistic refinement and grammatical correction. Following the application of these tools, the author(s) comprehensively reviewed, verified, and edited the resulting text. The author(s) maintain full accountability and responsibility for the accuracy, integrity, and final content of the publication.

References:

[1] J. Yang, C. Sha, X. Wang, H. Yang, Experimental investigation of vortex generator influence on wind turbine airfoil aerodynamic performance under turbulent inflow conditions, Acta Aerodynamica Sinica , 43, 5,31-40. (2025). DOI: 10.7638/kqdlxxb-2024.0227.

[2] X. Li, Ke Yang, X. Wang, Experimental and numerical analysis of the effects of vortex generator height on vortex characteristics and airfoil aerodynamic performance, *Energies* 2019, *12*(5), 959; https:// doi.org/10.3390/en12050959.

[3] Q. Wang, X. Wang, P. Cheng, M Zuo, Y.Ni, Integrated optimization design of wind turbine airfoil and vortex generators. European Journal of Mechanics –B/Fluids, 120, 204568, (2026). https://doi.org/10.1016/j.euromechflu.2026.204568.

[4] Shan Ma, W Chu. H.Zhang, X. Li, Effect of modified micro-vortex generators on aerodynamic performance in a high –load cascade, Proceedings of the Institution of Engineers Part A Journal of Power and Energy, 233 (3), 309-323, (2018). DOI: 10.1177/ 0957650918 7900 18.

[5] H. Lee and D. J.. Lee, Wake impact on aerodynamic characteristics of horizontal axis wind turbine under yawed flow conditions, Renewable Energy, Elsevier, vol. 136(C), pages 383-392, (2019). DOI: 10.1016/j.renene.2018.12.126.

[6] Wik, E., and Shaw, S.T., "Numerical Simulation of Micro Vortex Generators," 2nd AIAA Flow Control Conference. June 28-July 1 2004, Portland, Oregon, AIAA 2004-2697. DOI: 10.2514/6.2004-2697.

[7] S.D. Juan, M.Julio, M.D. Julio, E.C. Mauricia: Experimental study of vortex generators effects on low Reynolds number airfoils in turbulent flow, Int. Journal of Aerodynamics, 2(1), 50-56, (2012). DOI: 10.1504/IJAD.2012.046539.

[8] Rinku Mukherjee, H. Palanivel, Prediction of Aerodynamic Behaviour of a 3D Rectangular Blade with Airfoil-Shaped Vortex Generators

By Modeling Wind Tunnel Data International Conference on Advanced Energy Simulation and Modeling Techniques (ICAESMT-26), Cannes, France, 2026, [Online]. https://academicresearchlibrary.com/abstract-detail/5447 (Accessed Date: March 20, 2026).

[9] F. Kaya, H. Akbiyik, Aerodynamic performance changes of an airfoil modified with biomimetic spiky-vortex generators. Physics of Fluids 37, 095175, (2025), https://doi.org/10. 1063/ 5.0282283.

[10] D. Nayak, s. jamkatel, K. Balaji, CK Akhil, Patel Ankit Kumar and S Saranya, Investigation of the combined injection and vortex generators method for Aerofoil performance enhancement. Int. J. of Aeronautical and Space Sciences, 27, 12188-1227, (2026). https://doi.org/10.1007/s42405-025-01032-3.

[11] De Tavernier, C. Ferreira, A. Vire, Controlling Dynamic Stall using vortex generators on a wind turbine,. Wind Energy 172, 1194-1211, (2021). DOI: 10.1016/j.renene.2021.03.019

[12] C.R. Kumar, R. Kanna, P. Gopal, S.K., Arumugam, Experimental and numerical analysis of vortex generators designed for utility vehicles, Archives of Thermodynamics, 44 (3), 217-240, (2023). DOI: 10.24425/ather.2023.147545.

[13] M. Ross and Z. Yao, Influence of vortex generator geometry on aerodynamic performance of airfoils. Energy Reports 8, 512–523 (2022). DOI: 10.1016/j.egyr.2022.01.077.

[14] R Ozkan, and M. Sardar, Aerodynamic design and optimization of a small-scale wind turbine blade using a novel artificial bee colony algorithm based on blade element momentum (ABC-BEM) theory,. Energy Converson and Mgt. DOI: 10.1016/j.enconman.2023.11693.

[15] D. Patel and A. Mehta, Experimental comparison of various passive flow control devices on NACA airfoils. J. Wind Eng. Ind. Aerodyn. 214, 104743 (2021). DOI: 10.1016/j.jweia.2021.104743.

[16] P. Wang, L Wang, . Huang, Rui Wu, Y Wang, The effects of vortex generators on the characteristics of the tip hydrofoil and the horizontal axis tidal turbine blade. Renewable Energ, 224, 120116, (2024). DOI: 10.1016/j.renene.2024.120116.

[17] Makota sato,Spatial arrangement of vortex-generator-type plasma actuator for separation control of airfoil flow. Physics of Fluids, 37 (1),015181,(2025). DOI: 10.1063/5.0245278.

[18] Paramesh T., T. Tenzin, Mohammad Sarwar, Ahmad Mujeeb Azizi, Habte Getaneh, Tamal Jana, Improvement of Aerodynamic Performance of NACA 2412 Airfoil using Active and Passive Control Techniques, WSEAS Transactions on Fluid Mechanics, 19, 200-207, (2024). DOI: 10.37394/232013.2024.19.20.

[19] N. Susan, R. O. Awichi, S. Kadedesya, A. O, Oyem, Application of Computational Fluid Dynamics in Simulation and Optimization of a Fluidized Sugar Bed Dryer, WSEAS Transactions on Heat and Mass Transfer, 18, , 286–295 (2023). DOI: 10.37394/232012.2023.18.25.

Contribution of Individual Authors to the Creation of a Scientific Article (Ghostwriting Policy)

Yagya Dutta Dwivedi has developed the concept and carried out the modelling, simulation and the result analysis.

Anwar Baig has organized, drafted and executed the work.

Sources of Funding for Research Presented in a Scientific Article or Scientific Article Itself

No funding was received for conducting this study.

Conflict of Interest

The authors have no conflicts of interest to declare that are relevant to the content of this article.

Creative Commons Attribution License 4.0 (Attribution 4.0 International, CC BY 4.0)

This article is published under the terms of the Creative Commons Attribution License 4.0
https://creativecommons.org/licenses/by/4.0/deed.en_US